

## Article

# Effects of Meteorological Factors and Water-Nitrogen Management Techniques on Carbon Dioxide Fluxes in Wheat Fields in a Dry Semi-Humid Area

Xiangcheng Ma <sup>1,2,3</sup>, Mengfan Lv <sup>1,2,3</sup>, Tie Cai <sup>1,2,3,\*</sup> and Zhikuan Jia <sup>1,2,3,\*</sup><sup>1</sup> College of Agronomy, Northwest A&F University, Yangling, Xianyang 712100, China<sup>2</sup> Institute of Water-Saving Agriculture in Arid Areas of China, Northwest A&F University, Yangling, Xianyang 712100, China<sup>3</sup> Key Laboratory of Crop Physi-Ecology and Tillage Science in Northwestern Loess Plateau, Ministry of Agriculture, Northwest A&F University, Yangling, Xianyang 712100, China

\* Correspondence: caitie@nwsuaf.edu.cn (T.C.); jiazhk@126.com (Z.J.); Tel.: +86-029-87080168 (Z.J.)

**Abstract:** Studying carbon dioxide fluxes in wheat fields is becoming increasingly important. The dry semi-humid area in China is an important wheat production area, but the variations in carbon dioxide fluxes in wheat fields and the mechanisms associated with the carbon dioxide flux response to meteorological factors and water-nitrogen management have rarely been studied systematically in this area. Thus, we conducted a monitoring experiment in order to clarify the responses of CO<sub>2</sub>-C fluxes to meteorological factors and water-nitrogen management in wheat fields in this dry semi-humid area, and modeled the relationships between CO<sub>2</sub>-C fluxes and meteorological factors under different water-nitrogen managements. Four water-nitrogen treatments were tested in wheat fields: rain-fed (no water and nitrogen added), irrigation (150 mm water added), rain-fed plus nitrogen application (225 kg ha<sup>-1</sup> nitrogen added), and irrigation plus nitrogen application (150 mm water and 225 kg ha<sup>-1</sup> nitrogen added). The CO<sub>2</sub>-C fluxes and meteorological indicators were monitored and analyzed, before fitting the relationships between them. The direct and total effects of precipitation, air temperature, and water vapor pressure on CO<sub>2</sub>-C fluxes in wheat fields were all positive, and their total effect coefficients were more than 0.7 and significant. Irrigation and nitrogen application increased the CO<sub>2</sub>-C fluxes in wheat fields by 6.82–14.52% and 51.59–55.94%, respectively. The fitting results showed that partial least squares regression models of the relationships between meteorological factors and CO<sub>2</sub>-C fluxes in wheat fields under different treatments were all effective, with R<sup>2</sup>Y (cum) and Q<sup>2</sup> (cum) values around 0.7. Overall, these results suggest that precipitation, air temperature, water vapor pressure, and water and nitrogen addition have positive effects on CO<sub>2</sub>-C fluxes from wheat fields in dry semi-humid areas. The partial least squares regression method is also suitable for modeling the relationships between meteorological factors and CO<sub>2</sub>-C fluxes. These results may provide a scientific basis for predicting and regulating CO<sub>2</sub>-C fluxes in wheat fields in dry semi-humid areas, and provide a methodological reference for ecosystem carbon dioxide flux simulation studies.

**Keywords:** carbon dioxide flux; meteorological variable; partial least squares regression; path analysis; prediction model; water and nitrogen management



**Citation:** Ma, X.; Lv, M.; Cai, T.; Jia, Z. Effects of Meteorological Factors and Water-Nitrogen Management Techniques on Carbon Dioxide Fluxes in Wheat Fields in a Dry Semi-Humid Area. *Agronomy* **2023**, *13*, 1925. <https://doi.org/10.3390/agronomy13071925>

Academic Editor: Wei Zhang

Received: 9 June 2023

Revised: 18 July 2023

Accepted: 19 July 2023

Published: 20 July 2023



**Copyright:** © 2023 by the authors. Licensee MDPI, Basel, Switzerland. This article is an open access article distributed under the terms and conditions of the Creative Commons Attribution (CC BY) license (<https://creativecommons.org/licenses/by/4.0/>).

## 1. Introduction

Carbon is increasingly flowing into the atmospheric carbon pool, where atmospheric CO<sub>2</sub> concentration in 2019 increased to 410 ppm [1,2]. This increase in atmospheric carbon will lead to increased global warming and frequent meteorological disasters, thereby posing severe challenges to global development [1,3]. Agriculture is considered one of the most important sources of carbon dioxide emissions [4,5]. The microbial decomposition of soil organic matter, the respiratory metabolism of crop roots, and the mineralization of soil

organic matter are important processes in the conversion of agricultural soil carbon to atmospheric carbon [2,3,6]. Agriculture is also threatened by severe reductions in farmland carbon pools and the frequent occurrence of extreme climate events caused by carbon dioxide emissions [3,6]. Monitoring and studying agricultural carbon dioxide emissions can provide a theoretical basis for coping with global climate change and ensuring the healthy development of agriculture, and it has become one of the most important issues in the world.

Exploring the factors that influence carbon dioxide emissions and understanding their relationships has always been a major focus of research into agricultural carbon dioxide emissions [2,7–11]. Agricultural production relies on natural water, light, and heat resources, and thus agricultural carbon dioxide emissions are closely related to meteorological factors [9,10,12]. Air temperature and precipitation can regulate the carbon cycle process by affecting plant growth and soil properties, and they are considered to be important factors that drive carbon dioxide emissions [3,9,12,13]. The water vapor status in the air (relative humidity, water vapor pressure, vapor pressure deficit, etc.) and light status (sunshine duration, solar radiation, photosynthetically active radiation, etc.) can affect plant stomatal conductance, the photosynthetic level, and soil hydrothermal dynamics, which may have complex effects on carbon dioxide emissions [2,7,9,10,12–14]. Many previous studies have explored the total effects of various meteorological factors on agricultural carbon dioxide emissions, but their direct and indirect effects have rarely been considered and they require further analysis. Constructing a model based on the effects of meteorological factors on carbon dioxide emissions is helpful for applying abundant meteorological data to predicting and evaluating agricultural carbon dioxide emissions [14]. However, few modeling studies have addressed this problem, and thus further research is required. In addition, the samples that can be used for modeling often vary under different research conditions, so modeling methods with strong sample inclusiveness are more appropriate. The partial least squares regression (PLS) method is particularly advantageous, but it is rarely used in agricultural carbon dioxide flux modeling research and should be introduced.

Agricultural production also relies on anthropogenic inputs of water and nitrogen resources [15–18], so agricultural carbon dioxide emissions are also regulated by water and nitrogen management techniques [10,19,20]. Irrigation has diverse regulatory effects on carbon dioxide emissions by affecting soil aeration, microbial activity, and plant growth [8,21]. Nitrogen application can regulate carbon dioxide emissions by affecting plant root growth and the soil microbial community composition, and these regulatory effects vary under different conditions [10,22–24]. Therefore, the effects of water and nitrogen management on agricultural carbon dioxide emissions need to be further studied. In addition, both water and nitrogen management and meteorological factors have effects on agricultural carbon dioxide emissions, but few studies have considered them simultaneously, so there is a need to study them together.

Wheat is the grain crop with the largest planting area throughout the world, with about 220 million hectares [25], and thus carbon dioxide emissions from wheat fields are an important part of agricultural carbon dioxide emissions. Due to its high environmental adaptability and relatively low water requirements, wheat is one of the main cereal crops grown in the dry semi-humid area of China (more than 15.3 million hectares of arable land in this area) [26–29]. However, relatively few studies have investigated carbon dioxide emissions from wheat fields in this dry semi-humid area. The inter-monthly distribution of precipitation in this area is uneven due to the influence of the monsoon climate, and agricultural production is often threatened by the occurrence of drought [30]. Decreased precipitation due to climate warming will lead to more severe water shortages in agriculture [30]. In addition, the farmland in this area is threatened by soil degradation [31], and carbon dioxide emission processes can affect soil carbon pools and the quality of farmland. Therefore, it is very important to study the carbon dioxide emissions from wheat

fields in this area in the context of the increasing atmospheric carbon concentration and global warming.

Thus, we conducted experiments with different water and nitrogen treatments in wheat fields in the dry semi-humid study area and monitored CO<sub>2</sub>-C fluxes and meteorological indicators. The aims of this study were: (1) to determine the characteristic changes in meteorological factors and CO<sub>2</sub>-C fluxes; (2) to explore the effects of water and nitrogen management techniques and meteorological factors on CO<sub>2</sub>-C fluxes; and (3) to model the relationships between CO<sub>2</sub>-C fluxes and meteorological factors. We aimed to provide a scientific basis for reducing emissions from wheat fields and improving the quality of farmland in the dry semi-humid study area, and to provide a methodological and technical reference for predicting agricultural carbon dioxide emissions in further studies.

## 2. Materials and Methods

### 2.1. Experimental Site Description

The experiment was conducted at the Institute of Water-Saving Agriculture in Arid Areas of China (longitude 108°04' E, latitude 34°17' N; altitude 506 m), located on Guanzhong Plain. In the dry semi-humid study area, the annual average temperature, total solar radiation, and precipitation were 13.0 °C, 4800 MJ m<sup>-2</sup>, and 600 mm, respectively. The experimental field was flat. The soil in the field was Lou soil, which is classified as Eum-Orthric Anthrosol. Before starting the experiment, the basic properties of the soil (0–40 cm) were as follows: bulk density = 1.25 g cm<sup>-3</sup>, soil organic matter = 12.55 g kg<sup>-1</sup>, total nitrogen = 0.72 g kg<sup>-1</sup>, total potassium = 11.48 g kg<sup>-1</sup>, and total phosphorus = 0.69 g kg<sup>-1</sup>.

### 2.2. Experimental Design and Implementation

The experiment was conducted for three winter wheat growing seasons (October 2018 to June 2021) using a randomized block design with three blocks and the following four treatments: rain-fed (R), irrigation (I), rain-fed plus nitrogen application (RN), and irrigation plus nitrogen application (IN). The rain-fed treatments were dependent on natural precipitation. The treatments requiring irrigation were irrigated with 75 mm water at the early overwintering stage and jointing stage for wheat (total 150 mm water). In the treatments requiring nitrogen application, 225 kg ha<sup>-1</sup> of pure nitrogen (using urea) was applied before sowing wheat. The application amounts of phosphorus and potassium fertilizer in each treatment were consistent, with basal application rates of 75 kg ha<sup>-1</sup> P<sub>2</sub>O<sub>5</sub> (using calcium superphosphate) and 150 kg ha<sup>-1</sup> K<sub>2</sub>O (using potassium chloride) before sowing wheat. Xinong 979 (the main local wheat variety) was used as the test material, and artificial drilling and harvesting were conducted around October 20 each year and early June in the following year, respectively. The wheat row spacing was 20 cm and basic seedlings of 2.25 million plants ha<sup>-1</sup> were maintained in all plots. The plot area was 7.2 m<sup>2</sup> (3.0 m × 2.4 m). In order to prevent interference by water and fertilizer between plots, the plots were separated by 1 m wide walkways. Other management measures in the experimental field were consistent with local production practices. After wheat harvesting, the field was fallow in summer and uniformly tilled before autumn sowing.

### 2.3. Indicator Monitoring Methods

#### 2.3.1. CO<sub>2</sub>-C Flux Measurement

CO<sub>2</sub>-C flux sampling was conducted in wheat fields by using the static chamber method. The static chamber comprised a top box and base made of polyvinyl chloride and stainless steel, respectively, with dimensions of 40 cm × 30 cm × 40 cm and 40 cm × 30 cm × 15 cm. The top box was wrapped with heat-insulating reflective material and equipped with a thermometer and gas sampling pipe. The lower part of the base was a fixed frame (in the soil) and the upper part was a groove. The long side of the base was perpendicular to the planting row and the area covered by the base included the planting row and inter-row areas. Monitoring began after fertilization and sowing, and gas samples were collected every 5 days for the first half a month and then every half a month until

the wheat was harvested. Gas samples were always collected at 8:00–11:00 a.m. The top box was connected to the base groove and the seam was sealed with water, before extracting well-mixed gas samples using syringes at intervals of 0, 10, 20, and 30 min, and the temperature was also recorded. The CO<sub>2</sub> concentrations were determined in the samples by using a GC-2010 Plus gas chromatograph (Shimadzu, Kyoto, Japan). The CO<sub>2</sub>-C fluxes were calculated according to Formula (1) [32]:

$$F = k \times \frac{273.15}{T} \times H \times \frac{\Delta c}{\Delta t} \times 24 \tag{1}$$

where F is the CO<sub>2</sub>-C flux (mg m<sup>-2</sup> d<sup>-1</sup>), k is taken as 0.536 (kg C m<sup>-3</sup>), T is the mean temperature inside the static chamber (K), H is the height of the sampling box (m), Δc/Δt is the rate of change in the CO<sub>2</sub> concentration (ppm h<sup>-1</sup>), and 24 is the conversion factor (h d<sup>-1</sup>). Δc/Δt was estimated with linear regression analysis, and flux value was accepted when r > 0.95. Cumulative CO<sub>2</sub>-C emissions were estimated by integrating the monthly average CO<sub>2</sub>-C fluxes during the wheat growing season [33].

### 2.3.2. Meteorological Factor Monitoring

The detailed precipitation, air temperature, water vapor pressure, relative humidity, and sunshine duration data required for the study were obtained from the Yangling National General Weather Station. This station is located at the Institute of Water-Saving Agriculture in Arid Areas of China, about 200 m away from the experimental field. The station is used for the long-term continuous observation of meteorological data and service scientific experiments.

### 2.4. Statistical Analysis

Data from the 2018–2019 and 2020–2021 wheat growing seasons (complete monitoring) were used to analyze the relationships between CO<sub>2</sub>-C fluxes and meteorological factors, and to construct models. Data from the 2019–2020 wheat growing season (with some interruptions in CO<sub>2</sub>-C flux monitoring due to the pandemic) were used for model validation.

The direct and indirect relationships between the monthly scale y (average CO<sub>2</sub>-C flux) and x<sub>1</sub> (average air temperature (AT)), x<sub>2</sub> (average relative humidity (RH)), x<sub>3</sub> (average water vapor pressure (WVP)), x<sub>4</sub> (average daily precipitation (P)), and x<sub>5</sub> (average daily sunshine duration (SD)) were determined with path analysis. The relationships between y and x<sub>i</sub> are shown in Table 1. In Table 1, b<sub>i</sub> is the direct effect coefficient of x<sub>i</sub> on y, r<sub>ij</sub>\*b<sub>j</sub> is the indirect effect coefficient of x<sub>i</sub> on y through x<sub>j</sub>, r<sub>iy</sub> is the total effect coefficient of x<sub>i</sub> on y obtained by summing the direct and all indirect effect coefficients of x<sub>i</sub> on y, e refers to other factors that affect y, and R<sub>(i)</sub> is the decision coefficient representing the comprehensive determining effect of x<sub>i</sub> on y, which can be calculated using Formula (2) [34].

$$R_{(i)} = 2b_i \times r_{iy} - b_i^2 \tag{2}$$

**Table 1.** Path coefficients for effects of meteorological factors on CO<sub>2</sub>-C fluxes in wheat fields under different water and nitrogen treatments.

Factors	b <sub>i</sub>	r <sub>ij</sub> *b <sub>j</sub>					r <sub>iy</sub>	R <sub>(i)</sub>	R <sup>2</sup> and e
		AT	RH	WVP	P	SD			
AT	0.1412	-	-0.0122	0.4983	0.2798	-0.1206	0.7866	0.2022	
RH	-0.2373	0.0073	-	0.1133	0.1639	0.0865	0.1337	-0.1198	
WVP	0.5136	0.1370	-0.0523	-	0.3100	-0.0983	0.8100	0.5682	0.7717 and 0.4778
P	0.4108	0.0962	-0.0947	0.3876	-	-0.0179	0.7820	0.4737	
SD	-0.2248	0.0757	0.0913	0.2246	0.0327	-	0.1994	-0.1402	

Table 1. Cont.

Factors	$b_i$	$r_{ij} * b_j$					$r_{iy}$	$R_{(i)}$	$R^2$ and $e$	
		AT	RH	WVP	P	SD				
I	AT	0.1410	-	-0.0106	0.5191	0.2435	-0.1277	0.7653	0.1959	0.7275 and 0.5220
	RH	-0.2063	0.0073	-	0.1180	0.1427	0.0916	0.1532	-0.1058	
	WVP	0.5350	0.1368	-0.0455	-	0.2698	-0.1041	0.7920	0.5612	
	P	0.3575	0.0960	-0.0823	0.4038	-	-0.0190	0.7560	0.4127	
	SD	-0.2381	0.0756	0.0794	0.2339	0.0285	-	0.1792	-0.1420	
RN	AT	0.0668	-	-0.0124	0.6892	0.1914	-0.1153	0.8197	0.1050	0.7815 and 0.4675
	RH	-0.2414	0.0034	-	0.1567	0.1121	0.0827	0.1135	-0.1131	
	WVP	0.7104	0.0648	-0.0532	-	0.2121	-0.0940	0.8400	0.6888	
	P	0.2810	0.0455	-0.0963	0.5361	-	-0.0171	0.7491	0.3420	
	SD	-0.2150	0.0358	0.0929	0.3106	0.0224	-	0.2467	-0.1523	
IN	AT	0.0415	-	-0.0123	0.7340	0.1578	-0.1176	0.8034	0.0650	0.7433 and 0.5067
	RH	-0.2386	0.0021	-	0.1669	0.0924	0.0844	0.1072	-0.1081	
	WVP	0.7565	0.0403	-0.0526	-	0.1748	-0.0959	0.8231	0.6731	
	P	0.2316	0.0283	-0.0952	0.5710	-	-0.0175	0.7182	0.2790	
	SD	-0.2194	0.0223	0.0918	0.3308	0.0184	-	0.2439	-0.1552	

Note:  $b_i$ ,  $r_{ij} * b_j$ ,  $r_{iy}$ ,  $R_{(i)}$ , and  $e$  denote the direct effect coefficient, indirect effect coefficient, total effect coefficient, decision coefficient, and residual path coefficient, respectively. R represents rain-fed treatment (no water and nitrogen added); I represents irrigation treatment (150 mm water added); RN represents rain-fed plus nitrogen application treatment (225 kg ha<sup>-1</sup> nitrogen added); and IN represents irrigation plus nitrogen application treatment (150 mm water and 225 kg ha<sup>-1</sup> nitrogen added). WVP, RH, P, SD, and AT represent the monthly scale average water vapor pressure, average relative humidity, average daily precipitation, average daily sunshine duration, and average air temperature, respectively.

The relationships between CO<sub>2</sub>-C fluxes and meteorological factors were modeled based on PLS. PLS maximizes the explained covariance between variables by extracting components that adequately reflect the original variable information from the set of variables, and the extracted components are then used to construct a predictive model for the response variable [35]. PLS is applicable to cases with obvious collinearity between independent variables and small sample sizes [36]. Variable importance in projection (VIP) is a variable screening metric based on PLS, which is used to measure the explanatory ability of the independent variable with respect to the dependent variable. An independent variable with a VIP value greater than 1.0 is considered important and an independent variable with a VIP value less than 0.5 is considered less influential [35]. The VIP value can be calculated using Formula (3) [36]:

$$VIP_i = \sqrt{p \times \sum_{h=1}^m Rd(Y; t_h) \times w_{hi}^2 / \sum_{h=1}^m Rd(Y; t_h)} \quad (3)$$

where  $VIP_i$  is the VIP value of the independent variable  $x_i$ ,  $p$  is the number of independent variables,  $m$  is the number of extracted components,  $t_h$  is the  $h$ -th extracted component,  $Rd(Y; t_h)$  is the explanatory ability of  $t_h$  with respect to the dependent variable  $Y$ , and  $w_{hi}$  is the weight of  $x_i$  on  $t_h$ , which reflects the marginal contribution of  $x_i$  to  $t_h$ .

The PLS model was selected based on  $R^2Y$  (cum) and  $Q^2$  (cum).  $R^2Y$  (cum) indicates the degree to which the model fits the dependent variable  $Y$ , and  $Q^2$  (cum) is a measure of the predictive ability of the model as assessed by cross-validation, and thus larger values of  $R^2Y$  (cum) and  $Q^2$  (cum) indicate better model performance [37]. By analyzing the observed and corresponding predicted values of the CO<sub>2</sub>-C fluxes during the 2019–2020 wheat growing season, the model was further validated using the correlation coefficient ( $r$ ), root mean square error (RMSE), and symmetric mean absolute percentage error (SMAPE). The values of  $r$ , RMSE, and SMAPE can be calculated using Formulas (4–6), respectively [38,39]:

$$r = \frac{\sum_{i=1}^n (y_i - \bar{Y}) \times (f_i - \bar{F})}{\sqrt{\sum_{i=1}^n (y_i - \bar{Y})^2} / \sqrt{\sum_{i=1}^n (f_i - \bar{F})^2}} \quad (4)$$

$$\text{RMSE} = \sqrt{\frac{1}{n} \times \sum_{i=1}^n (f_i - y_i)^2} \quad (5)$$

$$\text{SMAPE} = \frac{100\%}{n} \times \sum_{i=1}^n \frac{|f_i - y_i|}{(|f_i| + |y_i|)/2} \quad (6)$$

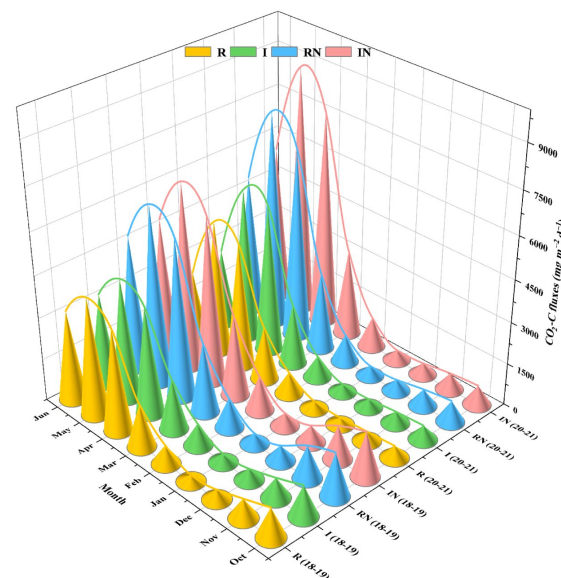
where  $n$  is the sample size,  $y_i$  is the  $i$ -th observed value,  $f_i$  is the  $i$ -th predicted value,  $Y$  is the average of the observed values, and  $F$  is the average of the predicted values. The performance of a model is better when  $r$  is closer to 1, SMAPE is farther away from 200%, and RMSE is smaller.

Path analysis was performed using SAS 8.1 (SAS, Cary, NC, USA). Collinearity between variables was analyzed using IBM SPSS Statistics 20 (IBM, Armonk, NY, USA). PLS analysis and model construction were performed with SIMCA 14.1 (UMETRICS, Umea, Sweden). The figures were prepared using OriginPro 2023 (OriginLab, Northampton, MA, USA).

### 3. Results

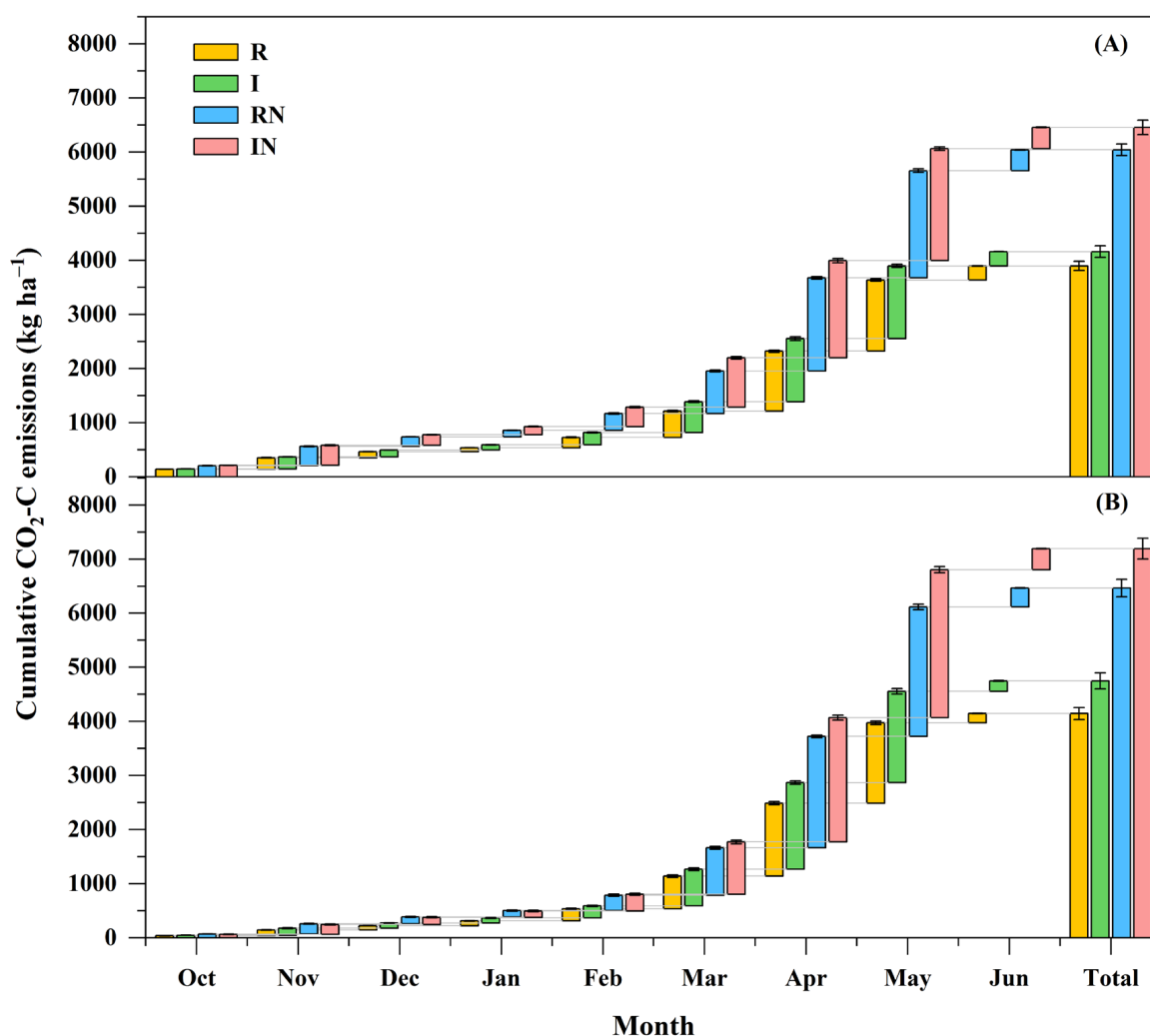
#### 3.1. Dynamics of CO<sub>2</sub>-C Fluxes in Wheat Fields

Figure 1 shows that the CO<sub>2</sub>-C fluxes in wheat fields under different water and nitrogen treatments exhibited similar seasonal patterns of variation during the wheat growing seasons, where they decreased initially, before increasing and finally decreasing. The CO<sub>2</sub>-C fluxes decreased to the lowest values in December–January (overwintering stage) and rose to the peak values in May (filling stage). Irrigation increased the average CO<sub>2</sub>-C fluxes in the wheat season under the same nitrogen level. The average CO<sub>2</sub>-C fluxes were 6.82–14.52% higher under I compared with R and 6.82–11.32% higher under IN compared with RN. Under the same water management pattern, the CO<sub>2</sub>-C fluxes in nitrogen-treated wheat fields were higher in all stages. The average CO<sub>2</sub>-C fluxes were 55.14–55.94% higher under RN compared with R and 51.59–55.15% higher under IN compared with I (Figure 1).



**Figure 1.** Dynamics of CO<sub>2</sub>-C fluxes under different water and nitrogen treatments in fields during the wheat growing seasons in 2018–2019 and 2020–2021. Note: R represents rain-fed treatment (no water and nitrogen added); I represents irrigation treatment (150 mm water added); RN represents rain-fed plus nitrogen application treatment (225 kg ha<sup>-1</sup> nitrogen added); and IN represents irrigation plus nitrogen application treatment (150 mm water and 225 kg ha<sup>-1</sup> nitrogen added). The Akima spline curve represents the trend in the CO<sub>2</sub>-C fluxes with time.

Figure 2 shows that April–May was the key period for CO<sub>2</sub>-C emissions from wheat fields, and the cumulative CO<sub>2</sub>-C emissions in this stage accounted for more than 60% of the cumulative CO<sub>2</sub>-C emissions in the whole wheat growing season. Under different water and nitrogen treatments, the cumulative CO<sub>2</sub>-C emissions in the wheat growing season were 3896.65–7195.28 kg ha<sup>-1</sup>. Irrigation increased the cumulative CO<sub>2</sub>-C emissions in the wheat growing season under the same nitrogen level. The cumulative CO<sub>2</sub>-C emissions were 264.04–602.71 kg ha<sup>-1</sup> higher under I compared with R and 413.57–730.41 kg ha<sup>-1</sup> higher under IN compared with RN. Nitrogen application also increased the cumulative CO<sub>2</sub>-C emissions in the wheat growing season under the same water management pattern. The cumulative CO<sub>2</sub>-C emissions were 2146.28–2320.86 kg ha<sup>-1</sup> higher under RN compared with R and 2295.81–2448.56 kg ha<sup>-1</sup> higher under IN compared with I (Figure 2).



**Figure 2.** Cumulative CO<sub>2</sub>-C emissions under different water and nitrogen treatments during the wheat growing seasons in 2018–2019 (A) and 2020–2021 (B). Note: the column length represents the mean  $\pm$  standard error for newly added cumulative CO<sub>2</sub>-C emissions in each stage.

### 3.2. Dynamics of Meteorological Factors

Figure 3 shows that the monthly variations in all meteorological factors (monthly averages) were relatively clear in the wheat growing season. The characteristic variations in WVP were basically the same in the two growing seasons, where it decreased initially and then increased, with a range of 3.0–16.0 hPa and the lowest period in December–January. The variations in RH were relatively complex and inconsistent in the two growing seasons, with a range of 46–76% (Figure 3). The variations in AT were similar to those in WVP, with

an overall “tick”-shaped trend and a range of 0.0–24.5 °C. The variations in SD differed greatly between the two growing seasons, with more abundant sunshine in the 2020–2021 growing season. The distributions of P were generally similar in the two growing seasons, with less in the early stage (drought in the winter and spring) and more in the late stage (Figure 3).

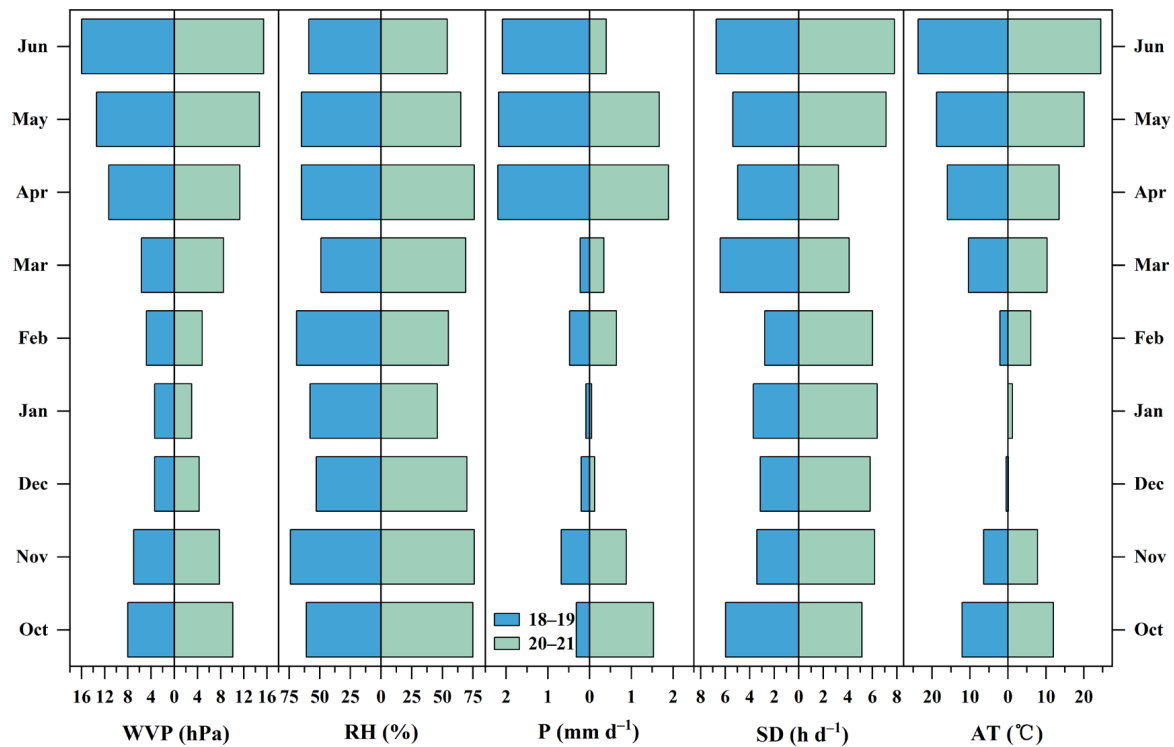


**Figure 3.** Dynamics of meteorological factors during the wheat growing seasons in 2018–2019 and 2020–2021. Note: WVP, RH, P, SD, and AT represent the monthly scale average water vapor pressure, average relative humidity, average daily precipitation, average daily sunshine duration, and average air temperature, respectively.

### 3.3. Responses of CO<sub>2</sub>-C Fluxes to Meteorological Factors

#### 3.3.1. Correlation Analysis

Figure 4 shows that the CO<sub>2</sub>-C fluxes under different water and nitrogen treatments were significantly positively correlated with AT and WVP, with correlation coefficients ranging from 0.765 to 0.820 and 0.792 to 0.840, respectively. Irrigation decreased the correlation coefficients between CO<sub>2</sub>-C fluxes and AT and WVP under the same nitrogen level, whereas nitrogen application increased the correlation coefficients between CO<sub>2</sub>-C fluxes and AT and WVP under the same water management pattern. Significant positive correlations were also found between the CO<sub>2</sub>-C fluxes and P under different water and nitrogen treatments, with correlation coefficients ranging from 0.718 to 0.782. Irrigation and nitrogen application both decreased the correlation coefficients between CO<sub>2</sub>-C fluxes and P (Figure 4). The CO<sub>2</sub>-C fluxes under different treatments were positively correlated (but not significantly) with RH and SD, with correlation coefficients ranging from 0.107 to 0.153 and 0.179 to 0.247, respectively. Under the same water management pattern, nitrogen application decreased the correlation coefficients between CO<sub>2</sub>-C fluxes and RH, but increased the correlation coefficients between CO<sub>2</sub>-C fluxes and SD (Figure 4). The responses of CO<sub>2</sub>-C fluxes to meteorological factors were influenced by the water and nitrogen management patterns.

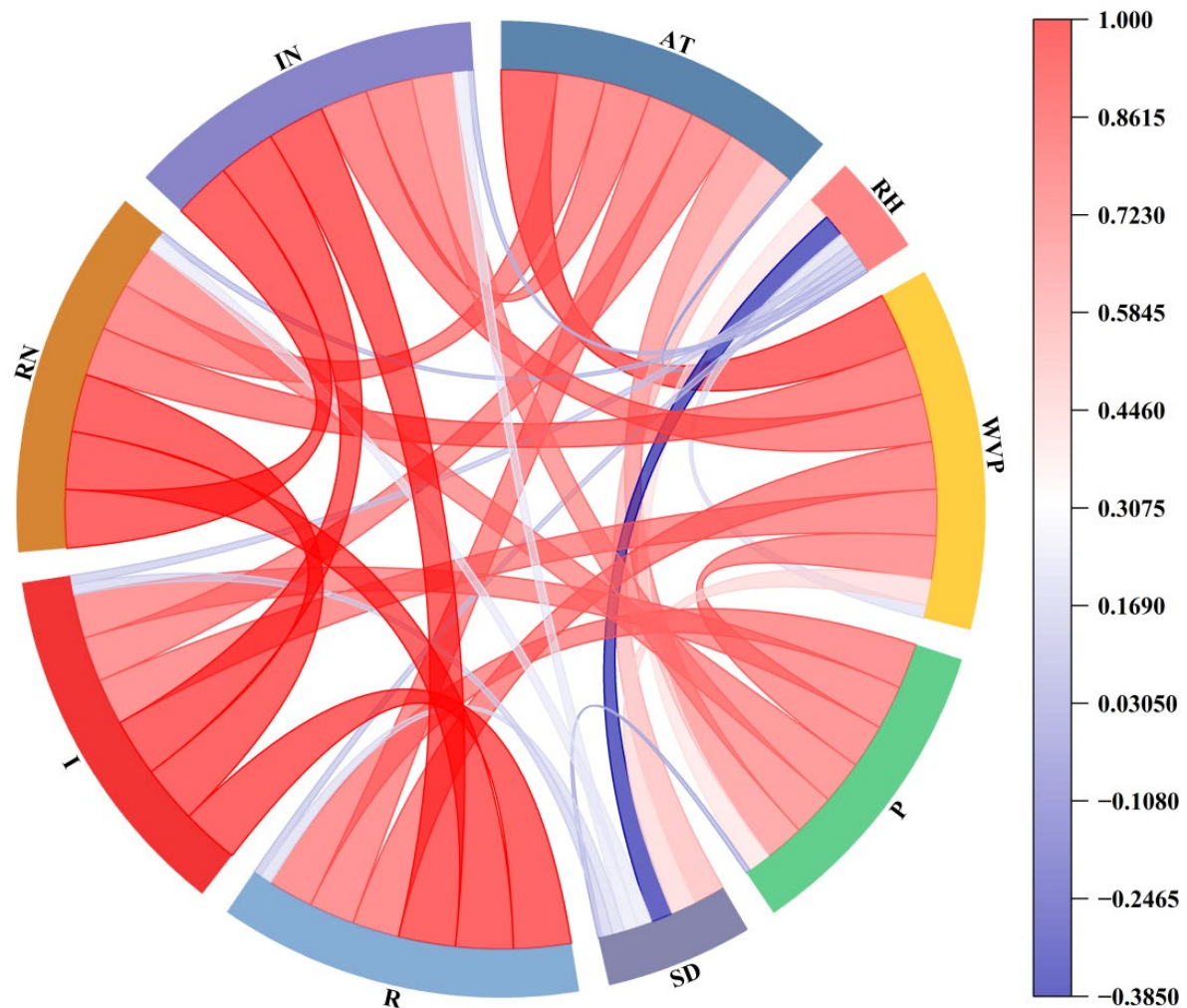


**Figure 4.** Correlations between meteorological factors and CO<sub>2</sub>-C fluxes in wheat fields under different water and nitrogen treatments. Note: the color of the connecting line represents the correlation coefficient value and the thickness of the connecting line represents the correlation degree.

### 3.3.2. Path Analysis

The effects of meteorological factors (AT, RH, WVP, P, and SD) on CO<sub>2</sub>-C fluxes could be explained effectively by path analysis, and the  $R^2$  values for the equations under each treatment were in the range of 0.7275–0.7815 (Table 1). Under different water and nitrogen treatments, the direct effects of RH and SD on CO<sub>2</sub>-C fluxes were negative and weak, whereas the direct effects of AT, WVP, and P on CO<sub>2</sub>-C fluxes were all positive. The direct effect coefficient of WVP was the largest (in the range of 0.5136–0.7565) under each treatment (Table 1). AT and P were significantly positively correlated with WVP (Figure 4), so the total effects of these three factors on CO<sub>2</sub>-C fluxes were all relatively large (Table 1). Under different water and nitrogen treatments, the  $R_{(i)}$  values for meteorological factors followed the order of WVP > P > AT > 0 > RH > SD (Table 1). Thus, WVP and P were the main decision variables, whereas RH and SD were restrictive variables. Both irrigation and nitrogen application decreased the direct and comprehensive determining effects of P on CO<sub>2</sub>-C fluxes, whereas both increased the direct effects of WVP on CO<sub>2</sub>-C fluxes. In addition, nitrogen application increased the comprehensive determining effects of WVP on CO<sub>2</sub>-C fluxes (Table 1).

### 3.4. Modeling Based on PLS Analysis

Figure 5 shows that the VIP values for meteorological factors were different, thereby indicating that they had different abilities to influence the CO<sub>2</sub>-C fluxes in wheat fields. Under different treatments, the VIP values were all greater than 1.0 for WVP, AT, and P, and the 95% confidence intervals for these VIP values did not contain 0. Thus, these three factors had significant effects on CO<sub>2</sub>-C fluxes. By contrast, the VIP values for SD and RH were less than 0.5, and the 95% confidence intervals for these VIP values contained 0, so the effects of SD and RH on CO<sub>2</sub>-C fluxes were not significant (Figure 5). Both irrigation and nitrogen application increased the VIP values for WVP and AT, but both decreased the VIP values for P (Figure 5). Table 2 shows that the variance inflation factor (VIF) values for AT and WVP were greater than 10 and their tolerance values were less than 0.1. Therefore, obvious collinearity was detected between AT and WVP.

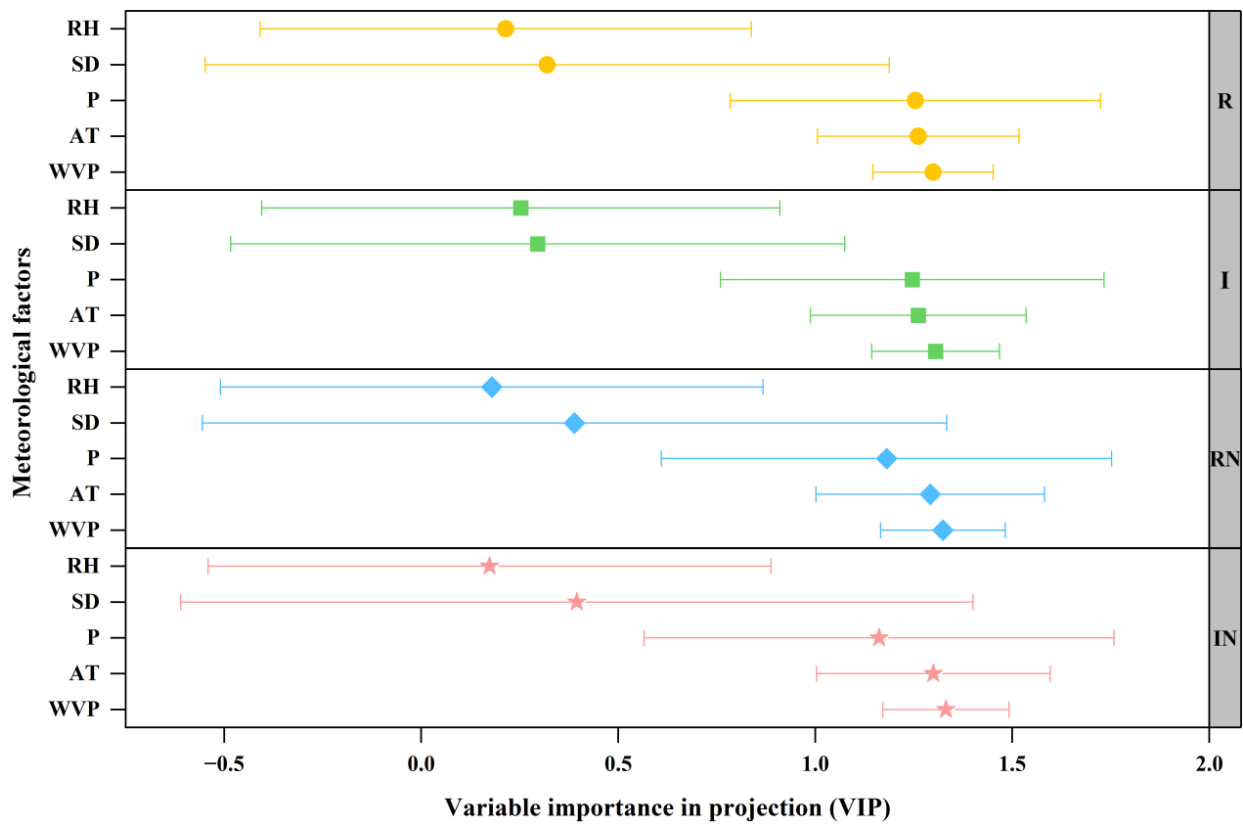


**Figure 5.** Variable importance in projection (VIP) values for the meteorological factors with respect to CO<sub>2</sub>-C fluxes in wheat fields under different water and nitrogen treatments. Note: Error bars represent 95% confidence intervals.

**Table 2.** Collinearity statistics for meteorological factors.

Meteorological Factors	Tolerance	VIF
AT	0.029	34.216
RH	0.446	2.244
WVP	0.027	37.079
P	0.342	2.926
SD	0.496	2.015

Note: VIF represents variance inflation factor.

Table 3 shows that different combinations of variables were formed by gradually removing meteorological factors with VIP values less than 0.5 and selectively removing (retaining at least one of them) meteorological factors with VIF values greater than 10, and

different models were constructed using the PLS method based on these combinations for optimal model selection. Under R and I, the models based on the combination of P and AT were optimal (with the largest R<sup>2</sup>Y (cum) and Q<sup>2</sup> (cum) values), and the models based on the combination of P, AT, and WVP were optimal under RN and IN (Table 3). The specific forms of the optimal models under each treatment are shown in Table 4.

**Table 3.** Performance of response models for wheat field CO<sub>2</sub>-C fluxes relative to different combinations of meteorological factors under different water and nitrogen treatments.

Model Number	Meteorological Factors	R		I		RN		IN	
		R <sup>2</sup> Y (cum)	Q <sup>2</sup> (cum)	R <sup>2</sup> Y (cum)	Q <sup>2</sup> (cum)	R <sup>2</sup> Y (cum)	Q <sup>2</sup> (cum)	R <sup>2</sup> Y (cum)	Q <sup>2</sup> (cum)
1	P, AT, WVP, RH, SD	0.696	0.669	0.659	0.626	0.715	0.684	0.679	0.641
2	P, AT, RH, SD	0.693	0.651	0.653	0.600	0.698	0.643	0.658	0.593
3	P, WVP, RH, SD	0.687	0.651	0.648	0.601	0.694	0.646	0.655	0.598
4	P, AT, WVP, RH	0.714	0.702	0.676	0.662	0.733	0.716	0.696	0.674
5	P, AT, WVP, SD	0.701	0.678	0.663	0.636	0.720	0.696	0.683	0.655
6	P, AT, WVP	0.724	0.714	0.684	0.675	0.743	0.731	0.704	0.690
7	P, AT, RH	0.714	0.698	0.672	0.652	0.719	0.692	0.678	0.645
8	P, AT, SD	0.701	0.668	0.659	0.618	0.704	0.665	0.664	0.618
9	P, WVP, RH	0.696	0.678	0.658	0.636	0.700	0.673	0.661	0.629
10	P, WVP, SD	0.704	0.676	0.664	0.629	0.708	0.675	0.668	0.628
11	P, AT	0.732	0.724	0.688	0.679	0.735	0.720	0.692	0.675
12	P, WVP	0.723	0.713	0.683	0.674	0.724	0.709	0.683	0.666

Note: R<sup>2</sup>Y (cum) indicates the degree to which the model fits the dependent variable, and Q<sup>2</sup> (cum) is a measure of the predictive ability of the model as assessed by cross-validation.

**Table 4.** Optimal partial least squares regression model under each water and nitrogen treatment.

	R		I		RN		IN	
	SC	UC	SC	UC	SC	UC	SC	UC
AT	0.468 # 0.124	95.297	0.455 # 0.144	102.214	0.314 # 0.090	100.678	0.308 # 0.104	108.605
WVP	-	-	-	-	0.322 # 0.069	190.014	0.315 # 0.085	204.925
P	0.465 # 0.151	952.450	0.450 # 0.137	1015.100	0.287 # 0.135	924.994	0.275 # 0.126	975.974
Const	1.075	-71.969	1.073	-21.553	1.078	-698.781	1.063	-717.445

Note: SC and UC represent standardized coefficients and unstandardized coefficients, respectively. # value represents the distance from the coefficient to the upper or lower limit of its 95% confidence interval.

### 3.5. Model Validation

Based on the P, AT, and WVP data during the 2019–2020 wheat growing season (Figure S1), the optimal model under each treatment was used to predict CO<sub>2</sub>-C fluxes. These predicted values were in good agreement with the corresponding observed values (Figure 6). The ranges of r, RMSE, and SMAPE were 0.985–0.993, 265.72–551.84 mg m<sup>-2</sup> d<sup>-1</sup>, and 16.40–22.78%, respectively (Table 5). Therefore, these results indicated the good performance of each optimal model.

**Table 5.** Validation results for the optimal model under each water and nitrogen treatment.

	r	RMSE (mg m <sup>-2</sup> d <sup>-1</sup> )	SMAPE
R	0.985	324.05	22.01%
I	0.988	265.72	16.40%
RN	0.993	551.84	22.78%
IN	0.989	517.40	19.29%

Note: r, RMSE, and SMAPE denote the correlation coefficient, root mean square error, and symmetric mean absolute percentage error, respectively.

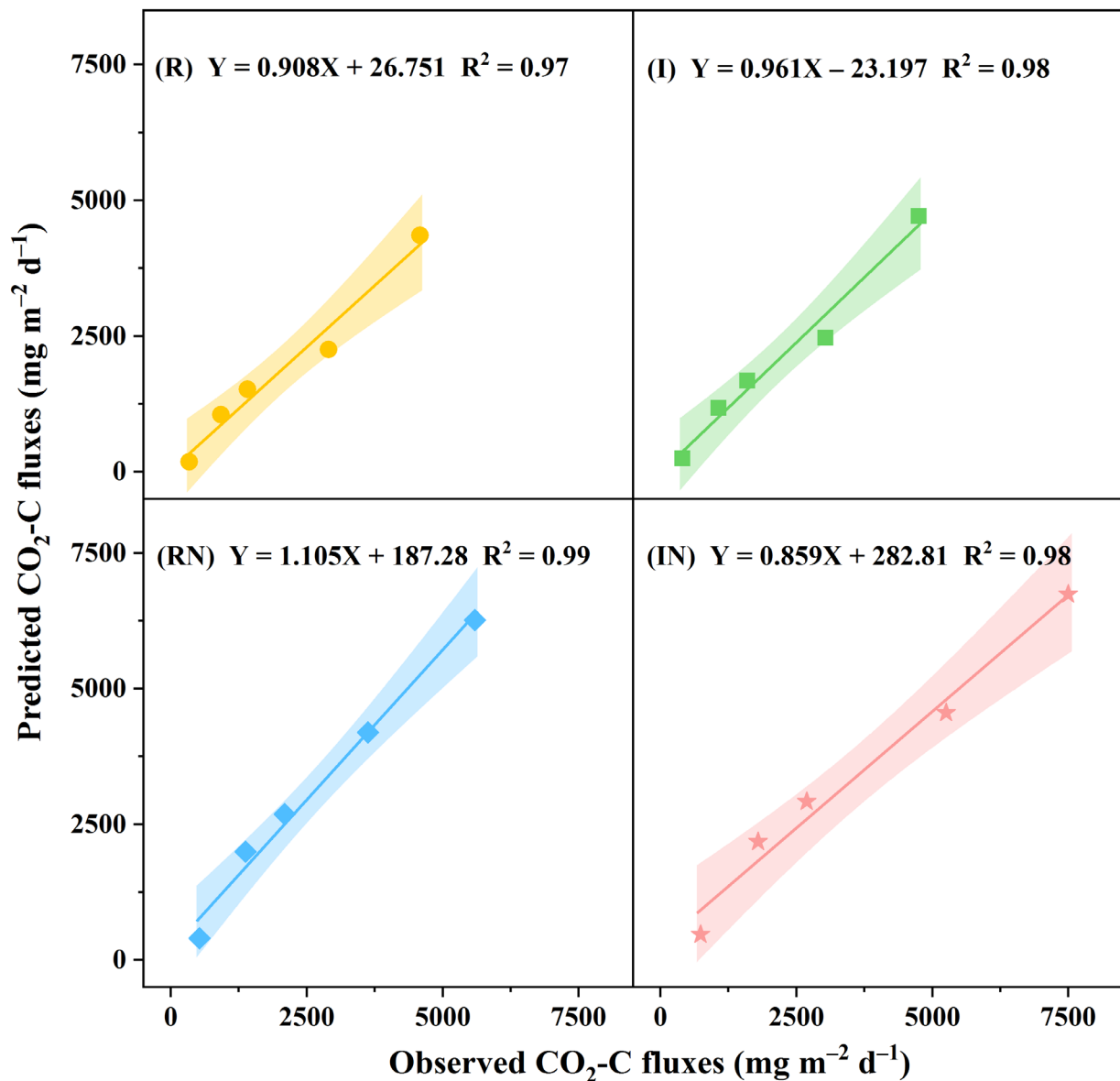


**Figure 6.** Observed and corresponding predicted values of field CO<sub>2</sub>-C fluxes under different water and nitrogen treatments during the 2019–2020 wheat growing season. Note: Shaded bands represent 95% confidence bands.

#### 4. Discussion

##### 4.1. Responses of Ecosystem Carbon Dioxide Fluxes to Meteorological Factors

Ecosystem CO<sub>2</sub> fluxes are often influenced by multiple meteorological factors [10,14,40]. Wang et al. [9] found that precipitation could affect the fluctuations in CO<sub>2</sub> fluxes in farmland ecosystems. Fatumah et al. [3] conducted experiments in banana–coffee farms in Uganda, and showed that precipitation was a key meteorological factor for regulating the carbon dioxide flux levels, and that the CO<sub>2</sub> fluxes increased as the precipitation increased. Similar to previous studies, the results obtained in the present study showed that precipitation was an important meteorological factor for regulating the variations in CO<sub>2</sub>-C fluxes in wheat fields, and it had a positive regulatory role. The positive regulatory effect of precipitation on farmland carbon dioxide fluxes may be explained by increasing precipitation improving the soil microbial activity, promoting the crop’s physiological metabolism, increasing the disturbance of the soil structure, and accelerating the soil pore gas efflux [3]. In addition, Golovatskaya and Dyukarev [41] found reliable relationships

between the air temperature and peat soil CO<sub>2</sub> fluxes at all time scales. Huang et al. [42] showed that carbon dioxide fluxes in plantation ecosystems in the hilly areas of north China increased as the monthly mean air temperature increased. Similar to previous studies, we found significant positive correlations between the air temperature and CO<sub>2</sub>-C fluxes in wheat fields. The positive regulatory effect of air temperature on ecosystem CO<sub>2</sub> fluxes may be explained by higher temperatures promoting soil microbial metabolism and soil organic carbon decomposition [10,43]. Furthermore, water vapor pressure, which is influenced by both precipitation and air temperature, is considered to have effects on water- or heat-dependent ecophysiological processes [44]. In the present study, water vapor pressure had significant positive effects on CO<sub>2</sub>-C fluxes in wheat fields.

However, the effects of the sunshine duration and relative humidity on ecosystem CO<sub>2</sub> fluxes are relatively complex. An increase in the sunshine duration can provide more light to promote plant photosynthetic carbon fixation [45], but also more heat to promote soil CO<sub>2</sub> emissions [7], and thus the sunshine duration can have diverse effects on ecosystem carbon cycling processes. Dhadli et al. [10] showed that the correlations between the sunshine duration and farmland CO<sub>2</sub> fluxes were not significant during the maize and wheat growing seasons. In the present study, the sunshine duration also had weak effects on CO<sub>2</sub>-C fluxes in wheat fields, with negative direct effects and positive total effects. In addition, the relative humidity can have diverse effects on ecosystem carbon cycling processes. Increased relative humidity can alleviate plant drought stress and increase stomatal conductance and photosynthetic carbon fixation [45,46], and higher relative humidity is not conducive to air flow, which has a limiting effect on ecosystem CO<sub>2</sub> emissions [47]. However, the improved moisture conditions associated with higher relative humidity may promote carbon metabolism in soil microbes and plant roots [14,48]. Melling et al. [49] found that relative humidity was the main regulatory factor for CO<sub>2</sub> fluxes in forest ecosystems, but it had less effect on CO<sub>2</sub> fluxes in crop cultivation systems, including no significant effect on CO<sub>2</sub> fluxes in sago cultivation systems. In the present study, the effects of relative humidity on CO<sub>2</sub>-C fluxes in wheat fields were also insignificant, with negative direct effects and positive total effects.

#### 4.2. Responses of Ecosystem Carbon Dioxide Fluxes to Water and Nitrogen Managements

Water is an important component of soil and an essential resource for plant growth and development, and water management can affect the soil properties and plant traits to regulate ecosystem CO<sub>2</sub> fluxes [50]. Jia et al. [51] found that water addition increased the soil CO<sub>2</sub> fluxes in bunge needlegrass grassland and purple alfalfa grassland in semi-arid areas. Similarly, Liu et al. [52] conducted experiments in spring maize fields on the Loess Plateau in China and showed that irrigation increased the soil CO<sub>2</sub> fluxes compared with rain-fed growing. Moreover, Sainju et al. [19] found that irrigation increased farmland carbon dioxide fluxes by 13% when increasing the soil water content in North Dakota, USA. Similar to previous studies, we found that irrigation increased the CO<sub>2</sub>-C fluxes by 6.82–14.52% in wheat fields in a dry semi-humid area. The increased ecosystem CO<sub>2</sub> fluxes under irrigation may be explained by the improved water conditions increasing the plant root activity, microbial metabolism, and substrate availability [51,52]. Furthermore, in the present study, we found that irrigation changed the effects of meteorological factors on CO<sub>2</sub>-C fluxes in wheat fields. Similarly, Liu et al. [52] showed that irrigation changed the relationships between meteorological factors and soil CO<sub>2</sub> fluxes in maize fields.

Nitrogen is an important nutrient that exists in many forms in soils and organisms, and it participates in a wide range of metabolic activities. Thus, nitrogen management can regulate the soil environment, microbial composition, and plant growth to affect ecosystem CO<sub>2</sub> fluxes [53,54]. Shao et al. [55] found that nitrogen application (90–360 kg N ha<sup>-1</sup>) increased carbon dioxide fluxes in winter wheat fields in northwest China. In addition, Sainju et al. [19] showed that nitrogen application increased the carbon dioxide fluxes in both conventional-till and no-till malt barley fields in North Dakota. Similar to previous studies, we found that nitrogen application increased the CO<sub>2</sub>-C fluxes in wheat fields

compared with no nitrogen application. The increased ecosystem CO<sub>2</sub> fluxes under nitrogen application may be explained by increases in soil fertility, soil microbial diversity, and the root biomass and exudates [10,24]. Furthermore, we found that nitrogen application changed the relationships between meteorological factors (precipitation, air temperature, water vapor pressure, etc.) and CO<sub>2</sub>-C fluxes in wheat fields to some extent. Similarly, Dhadli et al. [10] found that nitrogen application changed the effects of meteorological variables on farmland CO<sub>2</sub> fluxes.

#### *4.3. Modeling the Relationships between Ecosystem Carbon Dioxide Fluxes and Meteorological Factors*

Modeling the relationships between ecosystem CO<sub>2</sub> fluxes and meteorological factors can help to explain and predict changes in ecosystem CO<sub>2</sub> fluxes through meteorological data [14]. Constructing these models often involves identifying important independent variables and establishing response relationships between variables, and thus previous studies have introduced many relevant methods and explored their characteristics [10,12,38,56]. Dhadli et al. [10] used stepwise multiple linear regression analysis to model the relationships between farmland CO<sub>2</sub> fluxes and meteorological variables in Ludhiana, India, and showed that meteorological variables could explain 22–56% of the changes in farmland CO<sub>2</sub> fluxes through these models. This method can include both important variable screening and model construction, and it is simple and convenient to use. Qin et al. [56] used the Bayesian technique for automatic relevance determination to analyze the importance of input variables and modeled the response of carbon dioxide exchange to input variables in summer maize fields in the North China Plain region with the feed-forward back propagation neural network technique, and the predictive ability of this model was much better than that of the stepwise linear regression model. However, the use of the neural network technique to construct models is affected by problems such as difficulties in determining the network structure, explaining the model, and ensuring the reliability of the model under small sample sizes [56]. Cai et al. [38] modeled the response in terms of net ecosystem carbon exchange to environmental variables in evergreen needleleaf forest ecosystems in temperate oceanic climate regions using the gradient boosting regression method, and analyzed the importance of environmental variables using the random forest algorithm, which achieved good results. Gradient boosting regression improved the performance by combining a series of weak prediction models to form a strong prediction model, and this method has the advantages of accurate prediction, good stability, and widespread application [38]. However, the serial fitting of several weak prediction models by using this method may incur high computational overheads. The situations investigated in ecological and environmental studies are complex and diverse, and the availability of a small number of measurements is typical in ecology [56], which may demand applying modeling methods with strong sample size inclusiveness. The PLS method can be used in situations with low numbers of observed samples and it has great potential for application in the field of environmental monitoring [12]. In addition, the VIP metric based on this method can be used to measure the ability of the independent variable to explain the dependent variable [36], thereby helping to identify important variables conveniently and quickly. Yang et al. [12] used the PLS method to study the importance of each independent variable and to model the relationships between carbon dioxide exchange and meteorological variables in an apple orchard on the Loess Plateau, and good simulation and prediction results were obtained. Similarly, based on the experimental situation, we used the PLS method to effectively assess the ability of meteorological factors to explain CO<sub>2</sub>-C flux changes in wheat fields under different water and nitrogen treatments, and to successfully model the relationships between CO<sub>2</sub>-C fluxes and meteorological factors, where the R<sup>2</sup>Y (cum) and Q<sup>2</sup> (cum) values for the models were about 0.7.

## 5. Conclusions

The variations in CO<sub>2</sub>-C fluxes in wheat fields in a dry semi-humid area all exhibited a seasonal pattern, with decreases followed by increases and then decreases again under different water and nitrogen treatments. The precipitation, air temperature, and water vapor pressure were the most important meteorological factors that affected the variations in CO<sub>2</sub>-C fluxes in wheat fields, and their direct and total effects were positive. Irrigation and nitrogen application both increased the CO<sub>2</sub>-C fluxes in wheat fields, and also affected the relationships between CO<sub>2</sub>-C fluxes and meteorological factors. The PLS models of the relationships between meteorological factors and CO<sub>2</sub>-C fluxes in wheat fields all performed well under different water and nitrogen treatments. The results obtained in this study provide a scientific basis for the prediction and assessment of CO<sub>2</sub>-C fluxes, and for formulating emission reduction measures in wheat fields in dry semi-humid areas, as well as serving as a methodological reference for carbon dioxide flux simulation studies in other areas and ecosystems.

**Supplementary Materials:** The following supporting information can be downloaded at: <https://www.mdpi.com/article/10.3390/agronomy13071925/s1>, Figure S1: Meteorological data used for model validation during the 2019–2020 wheat growing season.

**Author Contributions:** Conceptualization, Z.J., T.C., and X.M.; methodology, T.C., X.M., and M.L.; investigation, X.M. and M.L.; data curation, Z.J., T.C., X.M., and M.L.; writing—original draft preparation, X.M.; writing—review and editing, Z.J., T.C., and X.M.; funding acquisition, Z.J. All authors have read and agreed to the published version of the manuscript.

**Funding:** This study was supported by the Program of the National Natural Science Foundation of China (No. 41671226).

**Data Availability Statement:** The data presented in this study are available within the article.

**Acknowledgments:** We are grateful to Junfeng Nie, Ruixia Ding, Hui Li, and Baoping Yang for help during the experimental period.

**Conflicts of Interest:** The authors declare no conflict of interest.

## References

1. IPCC. *Climate Change 2021: The Physical Science Basis. Contribution of Working Group I to the Sixth Assessment Report of the Intergovernmental Panel on Climate Change*; Cambridge University Press: Cambridge, UK; New York, NY, USA, 2021.
2. Liu, C.; Wu, Z.; Hu, Z.; Yin, N.; Islam, A.T.; Wei, Z. Characteristics and influencing factors of carbon fluxes in winter wheat fields under elevated CO<sub>2</sub> concentration. *Environ. Pollut.* **2022**, *307*, 119480. [[CrossRef](#)] [[PubMed](#)]
3. Fatumah, N.; Munishi, L.K.; Ndakidemi, P.A. Variations in greenhouse gas fluxes in response to short-term changes in weather variables at three elevation ranges, wakiso district, Uganda. *Atmosphere* **2019**, *10*, 708. [[CrossRef](#)]
4. Pratibha, G.; Srinivas, I.; Rao, K.; Shanker, A.K.; Raju, B.; Choudhary, D.K.; Rao, K.S.; Srinivasarao, C.; Maheswari, M. Net global warming potential and greenhouse gas intensity of conventional and conservation agriculture system in rainfed semi arid tropics of India. *Atmos. Environ.* **2016**, *145*, 239–250. [[CrossRef](#)]
5. Li, S.; Hu, M.; Shi, J.; Tian, X.; Wu, J. Integrated wheat-maize straw and tillage management strategies influence economic profit and carbon footprint in the Guanzhong Plain of China. *Sci. Total Environ.* **2021**, *767*, 145347. [[CrossRef](#)] [[PubMed](#)]
6. Lal, R.; Follett, R.F.; Stewart, B.A.; Kimble, J.M. Soil carbon sequestration to mitigate climate change and advance food security. *Soil Sci.* **2007**, *172*, 943–956. [[CrossRef](#)]
7. La Scala, N., Jr.; Panosso, A.; Pereira, G. Modelling short-term temporal changes of bare soil CO<sub>2</sub> emissions in a tropical agrosystem by using meteorological data. *Appl. Soil Ecol.* **2003**, *24*, 113–116. [[CrossRef](#)]
8. Jabro, J.; Sainju, U.; Stevens, W.; Evans, R. Carbon dioxide flux as affected by tillage and irrigation in soil converted from perennial forages to annual crops. *J. Environ. Manag.* **2008**, *88*, 1478–1484. [[CrossRef](#)]
9. Wang, W.; Liao, Y.; Wen, X.; Guo, Q. Dynamics of CO<sub>2</sub> fluxes and environmental responses in the rain-fed winter wheat ecosystem of the Loess Plateau, China. *Sci. Total Environ.* **2013**, *461*, 10–18. [[CrossRef](#)] [[PubMed](#)]
10. Dhadli, H.S.; Brar, B.; Black, T. Influence of crop growth and weather variables on soil CO<sub>2</sub> emissions in a maize-wheat cropping system. *Agric. Res. J.* **2015**, *52*, 28–34. [[CrossRef](#)]
11. He, X.; Du, Z.; Wang, Y.; Lu, N.; Zhang, Q. Sensitivity of soil respiration to soil temperature decreased under deep biochar amended soils in temperate croplands. *Appl. Soil Ecol.* **2016**, *108*, 204–210. [[CrossRef](#)]
12. Yang, J.; Duan, Y.; Yang, X.; Awasthi, M.K.; Li, H.; Zhang, L. Modeling CO<sub>2</sub> exchange and meteorological factors of an apple orchard using partial least square regression. *Environ. Sci. Pollut. Res.* **2020**, *27*, 43439–43451. [[CrossRef](#)] [[PubMed](#)]

13. Jiang, Y.; Wang, P.; Xu, X.; Zhang, J. Dynamics of carbon fluxes with responses to vegetation, meteorological and terrain factors in the south-eastern Tibetan Plateau. *Environ. Earth Sci.* **2014**, *72*, 4551–4565. [[CrossRef](#)]
14. Yue-Lin, L.; Otieno, D.; Owen, K.; Zhang, Y.; Tenhunen, J.; Xing-Quan, R.; Yong-Biao, L. Temporal variability in soil CO<sub>2</sub> emission in an orchard forest ecosystem. *Pedosphere* **2008**, *18*, 273–283.
15. Zhu, Z.; Chen, D. Nitrogen fertilizer use in China—Contributions to food production, impacts on the environment and best management strategies. *Nutr. Cycl. Agroecosyst.* **2002**, *63*, 117–127. [[CrossRef](#)]
16. Trost, B.; Prochnow, A.; Drastig, K.; Meyer-Aurich, A.; Ellmer, F.; Baumecker, M. Irrigation, soil organic carbon and N<sub>2</sub>O emissions. A review. *Agron. Sustain. Dev.* **2013**, *33*, 733–749. [[CrossRef](#)]
17. Yang, X.; Lu, Y.; Ding, Y.; Yin, X.; Raza, S. Optimising nitrogen fertilisation: A key to improving nitrogen-use efficiency and minimising nitrate leaching losses in an intensive wheat/maize rotation (2008–2014). *Field Crops Res.* **2017**, *206*, 1–10. [[CrossRef](#)]
18. Zhang, W.; He, X.; Zhang, Z.; Gong, S.; Zhang, Q.; Zhang, W.; Liu, D.; Zou, C.; Chen, X. Carbon footprint assessment for irrigated and rainfed maize (*Zea mays* L.) production on the Loess Plateau of China. *Biosyst. Eng.* **2018**, *167*, 75–86. [[CrossRef](#)]
19. Sainju, U.M.; Jabro, J.D.; Stevens, W.B. Soil carbon dioxide emission and carbon content as affected by irrigation, tillage, cropping system, and nitrogen fertilization. *J. Environ. Qual.* **2008**, *37*, 98–106. [[CrossRef](#)]
20. Hou, H.; Yang, Y.; Han, Z.; Cai, H.; Li, Z. Deficit irrigation effectively reduces soil carbon dioxide emissions from wheat fields in Northwest China. *J. Sci. Food Agric.* **2019**, *99*, 5401–5408. [[CrossRef](#)] [[PubMed](#)]
21. Sapkota, A.; Haghverdi, A.; Avila, C.C.; Ying, S.C. Irrigation and greenhouse gas emissions: A review of field-based studies. *Soil Syst.* **2020**, *4*, 20. [[CrossRef](#)]
22. Zhou, L.; Zhou, X.; Zhang, B.; Lu, M.; Luo, Y.; Liu, L.; Li, B. Different responses of soil respiration and its components to nitrogen addition among biomes: A meta-analysis. *Glob. Chang. Biol.* **2014**, *20*, 2332–2343. [[CrossRef](#)]
23. Mancinelli, R.; Marinari, S.; Brunetti, P.; Radicetti, E.; Campiglia, E. Organic mulching, irrigation and fertilization affect soil CO<sub>2</sub> emission and C storage in tomato crop in the Mediterranean environment. *Soil Tillage Res.* **2015**, *152*, 39–51. [[CrossRef](#)]
24. Qiu, W.; Liu, J.; Li, B.; Wang, Z. N<sub>2</sub>O and CO<sub>2</sub> emissions from a dryland wheat cropping system with long-term N fertilization and their relationships with soil C, N, and bacterial community. *Environ. Sci. Pollut. Res.* **2020**, *27*, 8673–8683. [[CrossRef](#)] [[PubMed](#)]
25. Zheng, Z.; Hoogenboom, G.; Cai, H.; Wang, Z. Winter wheat production on the Guanzhong Plain of Northwest China under projected future climate with SimCLIM. *Agric. Water Manag.* **2020**, *239*, 106233. [[CrossRef](#)]
26. Li, C.; Wang, C.; Wen, X.; Qin, X.; Liu, Y.; Han, J.; Li, Y.; Liao, Y.; Wu, W. Ridge–furrow with plastic film mulching practice improves maize productivity and resource use efficiency under the wheat–maize double–cropping system in dry semi–humid areas. *Field Crops Res.* **2017**, *203*, 201–211. [[CrossRef](#)]
27. Li, W.; Xiong, L.; Wang, C.; Liao, Y.; Wu, W. Optimized ridge–furrow with plastic film mulching system to use precipitation efficiently for winter wheat production in dry semi–humid areas. *Agric. Water Manag.* **2019**, *218*, 211–221. [[CrossRef](#)]
28. Igrejas, G.; Branlard, G. The importance of wheat. In *Wheat Quality for Improving Processing Human Health*; Igrejas, G., Ikeda, T.M., Guzmán, C., Eds.; Springer: Cham, Switzerland, 2020; pp. 1–7.
29. Wu, M.; Xu, Y.; Zheng, J.; Hao, Z. North Expansion of Winter Wheat Planting Area in China under Different Emissions Scenarios. *Agriculture* **2022**, *12*, 763. [[CrossRef](#)]
30. Hu, Y.; Ma, P.; Zhang, B.; Hill, R.L.; Wu, S.; Chen, G. Exploring optimal soil mulching for the wheat-maize cropping system in sub-humid drought-prone regions in China. *Agric. Water Manag.* **2019**, *219*, 59–71. [[CrossRef](#)]
31. Li, R.; Hou, X.; Jia, Z.; Han, Q. Soil environment and maize productivity in semi-humid regions prone to drought of Weibei Highland are improved by ridge-and-furrow tillage with mulching. *Soil Tillage Res.* **2020**, *196*, 104476. [[CrossRef](#)]
32. Beetz, S.; Liebersbach, H.; Glatzel, S.; Jurasinski, G.; Buczek, U.; Höper, H. Effects of land use intensity on the full greenhouse gas balance in an Atlantic peat bog. *Biogeosciences* **2013**, *10*, 1067–1082. [[CrossRef](#)]
33. Vera, J.C.; Acreche, M.M. Towards a baseline for reducing the carbon budget in sugarcane: Three years of carbon dioxide and methane emissions quantification. *Agric. Ecosyst. Environ.* **2018**, *267*, 156–164. [[CrossRef](#)]
34. Du, Y.; Du, J.; Liu, X.; Yuan, Z. Multiple-to-multiple path analysis model. *PLoS ONE* **2021**, *16*, e0247722. [[CrossRef](#)] [[PubMed](#)]
35. Levanoni, O.; Bishop, K.; Mckie, B.G.; Hartman, G.; Eklöf, K.; Ecke, F. Impact of beaver pond colonization history on methylmercury concentrations in surface water. *Environ. Sci. Technol.* **2015**, *49*, 12679–12687. [[CrossRef](#)]
36. Jia, Q.; Yu, W.; Zhou, L.; Liang, C. Atmospheric and surface-condition effects on CO<sub>2</sub> exchange in the Liaohe Delta Wetland, China. *Water* **2017**, *9*, 806. [[CrossRef](#)]
37. Obrador, B.; von Schiller, D.; Marcé, R.; Gómez-Gener, L.; Koschorreck, M.; Borrego, C.; Catalán, N. Dry habitats sustain high CO<sub>2</sub> emissions from temporary ponds across seasons. *Sci. Rep.* **2018**, *8*, 3015. [[CrossRef](#)] [[PubMed](#)]
38. Cai, J.; Xu, K.; Zhu, Y.; Hu, F.; Li, L. Prediction and analysis of net ecosystem carbon exchange based on gradient boosting regression and random forest. *Appl. Energy* **2020**, *262*, 114566. [[CrossRef](#)]
39. Chicco, D.; Warrens, M.J.; Jurman, G. The coefficient of determination R-squared is more informative than SMAPE, MAE, MAPE, MSE and RMSE in regression analysis evaluation. *PeerJ Comput. Sci.* **2021**, *7*, e623. [[CrossRef](#)]
40. Feiziene, D.; Feiza, V.; Vaideliene, A.; Povilaitis, V.; Antanaitis, S. Soil surface carbon dioxide exchange rate as affected by soil texture, different long-term tillage application and weather. *Agriculture* **2010**, *97*, 25–42.
41. Golovatskaya, E.; Dyukarev, E. The influence of environmental factors on the CO<sub>2</sub> emission from the surface of oligotrophic peat soils in West Siberia. *Eurasian Soil Sci.* **2012**, *45*, 588. [[CrossRef](#)]

42. Huang, H.; Zhang, J.; Meng, P.; Fu, Y.; Zheng, N.; Gao, J. Seasonal variation and meteorological control of CO<sub>2</sub> flux in a hilly plantation in the mountain areas of North China. *Acta Meteorol. Sin.* **2011**, *25*, 238–248. [[CrossRef](#)]
43. Hontoria, C.; Saa, A.; Rodríguez-Murillo, J. Relationships between soil organic carbon and site characteristics in peninsular Spain. *Soil Sci. Soc. Am. J.* **1999**, *63*, 614–621. [[CrossRef](#)]
44. Yin, X. Atmospheric water vapor pressure over land surfaces: A generic algorithm with data input limited to air temperature, precipitation and geographic location. *Theor. Appl. Climatol.* **1999**, *63*, 183–194. [[CrossRef](#)]
45. Driesen, E.; Van den Ende, W.; De Proft, M.; Saeyns, W. Influence of environmental factors light, CO<sub>2</sub>, temperature, and relative humidity on stomatal opening and development: A review. *Agronomy* **2020**, *10*, 1975. [[CrossRef](#)]
46. Talbott, L.D.; Rahveh, E.; Zeiger, E. Relative humidity is a key factor in the acclimation of the stomatal response to CO<sub>2</sub>. *J. Exp. Bot.* **2003**, *54*, 2141–2147. [[CrossRef](#)] [[PubMed](#)]
47. Song, X.; Yuan, H.; Kimberley, M.O.; Jiang, H.; Zhou, G.; Wang, H. Soil CO<sub>2</sub> flux dynamics in the two main plantation forest types in subtropical China. *Sci. Total Environ.* **2013**, *444*, 363–368. [[CrossRef](#)] [[PubMed](#)]
48. Mukhopadhyay, S.; Maiti, S. Soil CO<sub>2</sub> flux in grassland, afforested land and reclaimed coalmine overburden dumps: A case study. *Land Degrad. Dev.* **2014**, *25*, 216–227. [[CrossRef](#)]
49. Melling, L.; Hatano, R.; Goh, K.J. Soil CO<sub>2</sub> flux from three ecosystems in tropical peatland of Sarawak, Malaysia. *Tellus Ser. B-Chem. Phys. Meteorol.* **2005**, *57*, 1–11. [[CrossRef](#)]
50. Yan, L.; Chen, S.; Huang, J.; Lin, G. Differential responses of auto-and heterotrophic soil respiration to water and nitrogen addition in a semiarid temperate steppe. *Glob. Chang. Biol.* **2010**, *16*, 2345–2357. [[CrossRef](#)]
51. Jia, X.; Shao, M.; Wei, X. Soil CO<sub>2</sub> efflux in response to the addition of water and fertilizer in temperate semiarid grassland in northern China. *Plant Soil* **2013**, *373*, 125–141. [[CrossRef](#)]
52. Liu, Y.; Li, S.; Yang, S.; Hu, W.; Chen, X. Diurnal and seasonal soil CO<sub>2</sub> flux patterns in spring maize fields on the Loess Plateau, China. *Acta Agric. Scand. Sect. B-Soil Plant Sci.* **2010**, *60*, 245–255.
53. Wang, Y.; Cheng, S.; Fang, H.; Yu, G.; Xu, X.; Xu, M.; Wang, L.; Li, X.; Si, G.; Geng, J. Contrasting effects of ammonium and nitrate inputs on soil CO<sub>2</sub> emission in a subtropical coniferous plantation of southern China. *Biol. Fertil. Soils* **2015**, *51*, 815–825. [[CrossRef](#)]
54. Yan, W.; Zhong, Y.; Liu, J.; Shangguan, Z. Response of soil respiration to nitrogen fertilization: Evidence from a 6-year field study of croplands. *Geoderma* **2021**, *384*, 114829. [[CrossRef](#)]
55. Shao, R.; Deng, L.; Yang, Q.; Shangguan, Z. Nitrogen fertilization increase soil carbon dioxide efflux of winter wheat field: A case study in Northwest China. *Soil Tillage Res.* **2014**, *143*, 164–171. [[CrossRef](#)]
56. Qin, Z.; Su, G.; Zhang, J.; Ouyang, Y.; Yu, Q.; Li, J. Identification of important factors for water vapor flux and CO<sub>2</sub> exchange in a cropland. *Ecol. Model.* **2010**, *221*, 575–581. [[CrossRef](#)]

**Disclaimer/Publisher's Note:** The statements, opinions and data contained in all publications are solely those of the individual author(s) and contributor(s) and not of MDPI and/or the editor(s). MDPI and/or the editor(s) disclaim responsibility for any injury to people or property resulting from any ideas, methods, instructions or products referred to in the content.